

# Rainfall-runoff modelling by using SM2RAIN-derived and state-of-the-art satellite rainfall products over Italy

Luca Ciabatta<sup>1\*</sup>, Luca Brocca<sup>1</sup>, Christian Massari<sup>1</sup>, Tommaso Moramarco<sup>1</sup>

Simone Gabellani<sup>2</sup>

Silvia Puca<sup>3</sup>

Wolfgang Wagner<sup>4</sup>

<sup>1</sup>Research Institute for Geo-hydrological Protection, National Research Council, Perugia, Italy

<sup>2</sup>International Centre of Environmental Monitoring, Savona, Italy

<sup>3</sup>Civil Protection Department, Rome, Italy

<sup>4</sup>Department of Geodesy and Geoinformation, Vienna University of Technology, Vienna, Austria

Re-submitted to : International Journal of Applied Earth Observation and Geoinformation

July 2015

\* Luca Ciabatta, Research Institute for Geo-Hydrological Protection, National Research Council, Via Madonna Alta 126, 06128 Perugia, Italy. E-mail: [luca.ciabatta@irpi.cnr.it](mailto:luca.ciabatta@irpi.cnr.it).

1  
2  
3  
4  
5 1     **ABSTRACT**  
6

7  
8 2     Satellite rainfall products (SRPs) are becoming more accurate with ever increasing spatial and  
9  
10 3    temporal resolution. This evolution can be beneficial for hydrological applications, providing new  
11  
12  
13 4    sources of information and allowing to drive models in ungauged areas. Despite the large availability of  
14  
15 5    rainfall satellite data, their use in rainfall-runoff modelling is still very scarce, most likely due to  
16  
17 6    measurement issues (bias, accuracy) and the hydrological community acceptability of satellite  
18  
19  
20 7    products.  
21

22 8     In this study, the real-time version (3B42-RT) of Tropical Rainfall Measurement Mission Multi-  
23  
24  
25 9    satellite Precipitation Analysis, TMPA, and a new SRP based on the application of SM2RAIN  
26  
27 10   algorithm ([Brocca et al., 2014](#)) to the ASCAT (Advanced SCATterometer) soil moisture product,  
28  
29  
30 11   SM2R<sub>ASC</sub>, are used to drive a lumped hydrologic model over four basins in Italy during the 4-year  
31  
32 12   period 2010-2013.  
33

34 13     The need of the recalibration of model parameter values for each SRP is highlighted, being an  
35  
36  
37 14   important precondition for their suitable use in flood modelling. Results shows that SRPs provided, in  
38  
39 15   most of the cases, performance scores only slightly lower than those obtained by using observed data  
40  
41  
42 16   with a reduction of Nash-Sutcliffe efficiency (*NS*) less than 30% when using SM2R<sub>ASC</sub> product while  
43  
44 17   TMPA is characterized by a significant deterioration during the validation period 2012-2013.  
45  
46  
47 18   Moreover, the integration between observed and satellite rainfall data is investigated as well.  
48  
49 19   Interestingly, the simple integration procedure here applied allows obtaining more accurate rainfall  
50  
51  
52 20   input datasets with respect to the use of ground observations only, for 3 out 4 basins. Indeed, discharge  
53  
54 21   simulations improve when ground rainfall observations and SM2R<sub>ASC</sub> product are integrated, with an  
55  
56 22   increase of *NS* between 2 and 42% for the 3 basins in Central and Northern Italy. Overall, the study  
57  
58  
59  
60  
61  
62  
63  
64  
65

1  
2  
3  
4 highlights the feasibility of using SRPs in hydrological applications over the Mediterranean region with  
5  
6  
7 benefits in discharge simulations also in well gauged areas.  
8

9 **KEYWORDS:** Floods, rainfall, soil moisture, remote sensing, hydrological modelling.  
10

## 11 12 13 **1. INTRODUCTION** 14

15  
16 Floods are one of the most common and dangerous natural hazards, causing every year thousands  
17  
18 of casualties and damage worldwide ([Wake, 2013](#); [Jongman et al., 2014](#)). The main tool for assessing  
19  
20 flood risk and reducing damages is represented by hydrologic early warning systems that allow to  
21  
22 forecast flood events by using real time data obtained through ground monitoring networks (e.g.,  
23  
24 raingauges and radars, [Artan et al., 2007](#)). However, the use of such data, mainly rainfall, is affected by  
25  
26 many issues: 1) the limited spatial representativeness of local measurements ([Kidd et al., 2012](#)), 2) the  
27  
28 network density ([Rudolf and Schneider, 2005](#)) and 3) reflectivity issues related to meteorological  
29  
30 radars. A way to overcome these issues may be the use of satellite-based rainfall products (SRPs) that  
31  
32 nowadays are available on a global scale at ever increasing spatial/temporal resolution and accuracy.  
33  
34 For remote areas, SRPs are the only source of information ([Kidd and Levizzani, 2011](#)). Despite the  
35  
36 large availability of SRPs: e.g., the Tropical Rainfall Measurement Mission (TRMM) Multi-satellite  
37  
38 Precipitation Analysis (TMPA) ([Huffman et al., 2007](#)); the Satellite Application Facility on Support to  
39  
40 Operational Hydrology and Water Management (H-SAF, <http://hsaf.meteoam.it>, [Mugnai et al., 2013](#));  
41  
42 and the recent Global Precipitation Measurement (GPM) mission (<http://pmm.nasa.gov/GPM>, [Hou et](#)  
43  
44 [al., 2013](#)); remotely sensed rainfall data are scarcely used in hydrological modelling. Reasons may be  
45  
46 related to: 1) the inaccurate estimation of light rainfall that causes a general underestimation of the total  
47  
48 precipitation amounts, 2) the spatial/temporal resolution, 3) the timeliness, which is often insufficient  
49  
50 for operational purposes ([Serrat-Capdevilla et al., 2013](#)), and 4) the hydrological community  
51  
52 acceptability of satellite products. Indeed, in the scientific literature, only a small number of studies  
53  
54  
55  
56  
57  
58  
59  
60  
61  
62  
63  
64  
65

1  
2  
3  
46 were carried out, mainly concerning the hydrological validation of SRPs trying to outline some  
5  
6  
47 guidelines for using satellite data as input for hydrological modelling. By way of example, [Guetter et](#)  
8  
9  
48 [al. \(1996\)](#) simulated stream flow over three basins in America. They forced a rainfall-runoff-routing  
10  
11  
49 model by using a 10-year synthetic satellite rainfall dataset and carried out three different runs: 1) the  
12  
13  
14  
50 model was calibrated and validated with observed rainfall data; 2) the model was calibrated with  
15  
16  
51 observed rainfall data and then validated by using the synthetic satellite data; 3) the model was  
17  
18  
52 calibrated and validated with satellite data. They found an underestimation of the mean-areal  
20  
21  
53 precipitation and, hence, biased stream flow simulations when the model was calibrated with observed  
22  
23  
54 data and forced with the synthetic satellite dataset. They also found an increment of the errors as the  
24  
25  
55 basin area decreases. [Artan et al. \(2007\)](#) used the National Oceanic and Atmospheric Administration  
27  
28  
56 (NOAA) Climate Prediction Center (CPC) product for Famine Early Warning System (FEWS, [Xie and](#)  
29  
30  
31  
57 [Arkin, 1997](#)) to drive a physically-based semi-distributed hydrologic model over four basins in Asia  
32  
33  
58 and Africa. They found that SRPs can be used to force a hydrologic model provided that the  
34  
35  
59 recalibration of the model parameter values is carried out. [Harris et al. \(2007\)](#) used TMPA 3B42 real  
37  
38  
60 time product to drive a hydrologic model over a catchment in Kentucky finding that a bias correction is  
39  
40  
61 needed before using real-time satellite data in flood forecasting. [Stisen and Sandholt \(2010\)](#) forced a  
42  
43  
62 distributed hydrologic model over the Senegal River Basin with different SRPs: TMPA 3B42 V6,  
44  
45  
63 Climate Prediction Center MORPHing technique (CMORPH, [Joyce et al., 2004](#)), CPC FEWS v.2,  
47  
48  
64 Precipitation Estimation from Remotely Sensed Information using Artificial Neural Networks  
49  
50  
65 (PERSIANN, [Hsu et al., 1997](#))  
51  
52  
66 that the SRPs need a bias correction because of the differences in the estimates of the analyzed  
54  
55  
67 products (e.g., the number of rainy days and the recorded intensity). However, [Stisen and Sandholt](#)  
56  
57  
68 [\(2010\)](#) stated that satellite data can be very useful due to their spatial and temporal continuity and

1  
2  
3  
4  
5  
6  
7  
8  
9  
10  
11  
12  
13  
14  
15  
16  
17  
18  
19  
20  
21  
22  
23  
24  
25  
26  
27  
28  
29  
30  
31  
32  
33  
34  
35  
36  
37  
38  
39  
40  
41  
42  
43  
44  
45  
46  
47  
48  
49  
50  
51  
52  
53  
54  
55  
56  
57  
58  
59  
60  
61  
62  
63  
64  
65

should be considered to drive hydrologic models, mainly in remote and ungauged areas. [Thiemig et al. \(2013\)](#) performed a hydrological validation considering TMPA 3B42 v6, CMORPH, PERSIANN, the reanalysis product by the European Centre for Medium-range Weather Forecasting (ECMWF) ERA-Interim ([Dee et al., 2011](#)) and a local rainfall estimation calibrated over the African continent ([NOAA CPC, 2002](#)) over two basins in Africa. They pointed out that a model recalibration with each SRP and a bias correction are necessary in order to improve the stream flow simulations performance. To sum up, SRPs can be beneficially used for rainfall-runoff modelling but bias correction and model recalibration are required pre-processing steps.

The objective of this study is twofold. First, we aim to explore the feasibility of using SRPs in a lumped hydrologic model (MISDc, “Modello Idrologico Semi-Distribuito in continuo”, [Brocca et al., 2011b](#)) over 4 basins in Italy with different sizes and physiographic characteristics. Specifically, TMPA 3B42-RT and a new soil moisture (SM)-derived rainfall datasets obtained through the application of SM2RAIN algorithm ([Brocca et al., 2013b; 2014](#)) to ASCAT (Advanced SCATterometer) SM product are used in the analysis and the performances are compared with those obtained by using ground data during the 4-year period from 2010 to 2013. The analysis period is divided into a calibration (2010-2011) and a validation period (2012-2013). Second, we aim to investigate the integration between observed and satellite-based rainfall estimates in order to obtain more accurate and reliable rainfall datasets able to improve flood simulation with respect to the use of ground observation only.

## 2. MATERIALS AND METHODS

### 2.1 Study areas

Four basins throughout the Italian territory are considered in this analysis, specifically the Brenta, the Tanaro (Northern Italy), the Tiber (Center Italy) and the Volturno (Southern Italy) basins. The

1  
2  
3  
4  
5  
6  
7  
8  
9  
10  
11  
12  
13  
14  
15  
16  
17  
18  
19  
20  
21  
22  
23  
24  
25  
26  
27  
28  
29  
30  
31  
32  
33  
34  
35  
36  
37  
38  
39  
40  
41  
42  
43  
44  
45  
46  
47  
48  
49  
50  
51  
52  
53  
54  
55  
56  
57  
58  
59  
60  
61  
62  
63  
64  
65

elevation maps reported in *Figure 1*, and the main features listed in *Table 1*, highlight the differences between the basins: Tanaro is the biggest basin and is characterized by a mountainous area upstream and a large flood plain downstream. Brenta is the smallest one, mainly mountainous and it is characterized by the highest rainfall regime (see *Table 1*). These two first basins are characterized by mountainous areas where snow fall might occur during winter. Tiber basin is characterized by a quite large flood plain in the central area of the basin surrounded by hills and it has the lowest rainfall regime. Volturno basin is mainly flat with the presence of some low elevation mountains in the southern part of the basin. The basins are selected in four sectors of the Italian territory (North-Eastern, North-Western, Central and Southern Italy) in order to investigate different physiographic and climatic conditions. Moreover, basin selection is driven from the availability of good quality meteorological and discharge observations (based on the study by [Massari et al., 2015](#)), and from the suitability of the employed hydrological model, MISDc, as it does not incorporate a snow melting module.

## 2.2 Rainfall products

Ground-based rainfall, temperature and discharge data at hourly temporal resolution are provided by the Italian hydrometeorological network of the National Civil Protection Department. For a complete description of the observed dataset, the reader is referred to [Massari et al. \(2015\)](#). Specifically, the observed rainfall dataset is provided by the interpolation of more than 3000 raingauges throughout the Italian territory ([Ciabatta et al., 2015b](#)).

The SRPs considered in this study are the TMPA 3B42-RT product ([Huffman et al., 2007](#)), hereinafter TMPA, and the dataset obtained by applying the SM2RAIN algorithm ([Brocca et al., 2013b; 2014](#)) to the Advanced SCATterometer (ASCAT) SM data ([Wagner et al., 2013](#)), hereinafter SM2R<sub>ASC</sub>.

1  
2  
3  
4  
5  
6  
7  
8  
9  
10  
11  
12  
13  
14  
15  
16  
17  
18  
19  
20  
21  
22  
23  
24  
25  
26  
27  
28  
29  
30  
31  
32  
33  
34  
35  
36  
37  
38  
39  
40  
41  
42  
43  
44  
45  
46  
47  
48  
49  
50  
51  
52  
53  
54  
55  
56  
57  
58  
59  
60  
61  
62  
63  
64  
65

The TMPA product combines rainfall estimates from various satellite sensors. The multi-satellite platform uses TRMM Microwave Imager (TMI), the Special Sensor Microwave Imager (SSM/I) onboard Defense Meteorological Satellite Program (DMSP) satellites, the Advanced Microwave Scanning Radiometer-Earth Observing System (AMSR-E) and the Advanced Microwave Sounding Unit-B (AMSU-B) onboard the National Oceanic and Atmospheric Administration (NOAA) satellites. In addition, the TMPA product also uses geostationary (GEO) satellite infra-red (IR) data, characterized by higher spatial and temporal resolution than the Microwave (MW) sensors, through a constellation of GEO satellites. The TMPA product is provided by the National Aeronautics and Space Administration (NASA, <http://trmm.gsfc.nasa.gov/>) with a temporal resolution of 3 hours and a spatial resolution of 0.25° for the ± 50° North-South latitude band. Although a gauged corrected TMPA 3B42 product version is also available, in this study such product is not used in order to evaluate the feasibility of using SRPs in an operational framework, i.e., for real-time flood forecasting.

The second dataset is obtained by the application of the SM2RAIN algorithm ([Brocca et al., 2013b, 2014](#); [Ciabatta et al., 2015b](#)) to the Surface Soil Moisture (SSM) product obtained from ASCAT ([Wagner et al., 2013](#)), a scatterometer operating at 5.3 GHz onboard MetOp A and B satellites. Specifically, the Water Retrieval Package (WARP) 5.51 product is used in this study to estimate rainfall from SM data. The product has a resolution of 25 km (resampled at 12.5 km, [Wagner et al., 2013](#)) and is provided within the H-SAF project (<http://hsaf.meteoam.it>). For more details about SM2RAIN algorithm, the reader is referred to ([Brocca et al., 2013b, 2014](#); [Ciabatta et al., 2015b](#)), while a first application using the algorithm SM2RAIN for flood prediction through in situ SM data can be found in [Massari et al. \(2014\)](#). In this study, the same SM2RAIN-derived product as considered in [Ciabatta et al. \(2015a; 2015b\)](#) is employed.

1  
2  
3  
4  
5  
6  
7  
8  
9  
10  
11  
12  
13  
14  
15  
16  
17  
18  
19  
20  
21  
22  
23  
24  
25  
26  
27  
28  
29  
30  
31  
32  
33  
34  
35  
36  
37  
38  
39  
40  
41  
42  
43  
44  
45  
46  
47  
48  
49  
50  
51  
52  
53  
54  
55  
56  
57  
58  
59  
60  
61  
62  
63  
64  
65

Both SRPs and the observed rainfall data are remapped over a grid with spacing of 12.5 km, using the nearest neighbour algorithm. As described in [Ciabatta et al., \(2015b\)](#), the selected spacing is a compromise between the resolution of the different rainfall datasets and it was found to not significantly affect the results. The one day cumulated rainfall at 00:00 UTC+1 for each analysed dataset is considered in this study. Although TMPA data are provided within a time window  $\pm 90$  minutes from the nominal time (0000,0300,...,2100 UTC), all the remaining data are released in local time, i.e. UTC +1. This allows to compare TMPA data with the other datasets with only 30 minutes of delay.

In order to match the different temporal resolutions, the analysis is carried out at a daily time scale, and hence, the mean observed discharge, mean temperature and the accumulated rainfall during one day are computed and considered in the sequel.

### 2.2.1 Bias correction

In order to take into account the systematic errors due to the indirect measurement of rainfall by satellite sensors ([Kucera et al., 2013](#)), a bias correction is applied to each SRP. The applied correction allows to match the mean and the standard deviation of SRPs with the observed rainfall data. The correction applied in this study is expressed by:

$$P_{corr} = \left( \frac{P_{sat} - \overline{P_{sat}}}{\sigma_{sat}} \right) \sigma_{obs} + \overline{P_{obs}} \quad (1)$$

where  $P_{corr}$  is the bias corrected SRP,  $P_{sat}$  is the original SRP,  $\overline{P_{sat}}$  is the temporal mean of SRP,  $\sigma_{sat}$  is the standard deviation of SRP,  $\overline{P_{obs}}$  is the temporal mean of observed rainfall, and  $\sigma_{obs}$  is the standard deviation of observed rainfall. This formulation, originally applied by [Draper et al. \(2009\)](#) and [Brocca et al. \(2011a\)](#) to satellite SM data, is simple to implement in an operational framework and allows to correct the bias of SRPs. The correction is applied in the calibration period before the



1  
2  
3  
4  
5  
6  
7  
8  
9  
10  
11  
12  
13  
14  
15  
16  
17  
18  
19  
20  
21  
22  
23  
24  
25  
26  
27  
28  
29  
30  
31  
32  
33  
34  
35  
36  
37  
38  
39  
40  
41  
42  
43  
44  
45  
46  
47  
48  
49  
50  
51  
52  
53  
54  
55  
56  
57  
58  
59  
60  
61  
62  
63  
64  
65

computation of the mean areal rainfall. In the validation period, the same correction is applied without changing the correction coefficients.

### 2.2.2 Mean areal rainfall

The mean areal rainfall for each basin is obtained by considering the contribution of each pixel inside the basin by using the following equation:

$$P_A = \sum_{i=1}^N \frac{p_i a_i}{A_{tot}} \tag{2}$$

where  $P_A$  is the mean areal rainfall amount,  $p_i$  is the rainfall for the pixel  $i$  within a polygon of area  $a_i$  that represents the portion of the basin area covered by the pixel  $i$ , and  $A_{tot}$  is the total basin area.

### 2.2.3 Integration scheme

The integration of satellite and ground observed rainfall datasets is carried out by using the following nudging scheme:

$$P_{int}(t) = P_{sat}(t) + K[P_{obs}(t) - P_{sat}(t)] \tag{3}$$

where  $t$  is the time,  $P_{int}$  is the integrated rainfall,  $P_{sat}$  is the satellite rainfall,  $P_{obs}$  is the observed rainfall, and  $K$  is the weight factor that ranges between 0 and 1. For  $K=1$ , only the observed rainfall is considered, while for  $K=0$  only the satellite products are used as input into the model. The  $K$ -values are obtained through calibration, by maximizing the Nash-Sutcliffe efficiency index ( $NS$ ) between the observed and simulated discharge during the calibration period.

To sum up, a total of 5 different rainfall datasets are used in this study:

1. Observed rainfall (hereinafter OBS);
2. Bias corrected SM2RAIN-derived rainfall dataset (SM2R<sub>ASC</sub>);
3. Bias corrected TMPA 3B42-RT (TMPA);
4. Integrated rainfall dataset between OBS and SM2R<sub>ASC</sub> (hereinafter SM2R<sub>ASC</sub>+OBS);

1  
2  
3  
4  
5  
6  
7  
8  
9  
10  
11  
12  
13  
14  
15  
16  
17  
18  
19  
20  
21  
22  
23  
24  
25  
26  
27  
28  
29  
30  
31  
32  
33  
34  
35  
36  
37  
38  
39  
40  
41  
42  
43  
44  
45  
46  
47  
48  
49  
50  
51  
52  
53  
54  
55  
56  
57  
58  
59  
60  
61  
62  
63  
64  
65

5. Integrated rainfall dataset between OBS and TMPA (hereinafter TMPA+OBS).

### 2.3 MISDc rainfall-runoff model

The lumped version of the continuous and semi-distributed rainfall-runoff model MISDc (*Figure 2*), proposed by [Brocca et al. \(2011b; 2013a\)](#) is adopted here. MISDc is a single layer model and it was specifically developed for flood forecasting purposes, as a consequence it may have limitations in reproducing accurately the low flow conditions which in turn may determine volume errors in the long-term comparison between observed and simulated discharge. MISDc couples a routing module with a single layer soil water balance module ([Brocca et al., 2008](#)). Soil water balance is based on the following equation:

$$\frac{dW(t)}{dt} = [p(t) - p_e(t)] - e(t) - g(t) \quad (4)$$

where  $W(t)$  is the soil water content at time  $t$ ,  $p(t)$ ,  $p_e(t)$ ,  $e(t)$  and  $g(t)$  are the rainfall, effective rainfall, actual evapotranspiration and percolation rates, respectively. In *Equation (4)*,  $e(t)$  is calculated as a linear function between the potential evaporation, that is estimated via the Blaney and Criddle relation modified by [Doorembos and Pruitt, \(1977\)](#), and the soil saturation. The non-linear relation proposed by [Famiglietti and Wood \(1994\)](#) is used for the computation of the percolation rate,  $g(t)$ . The rainfall excess,  $p_e(t)$ , is calculated by using the well-known Soil Conservation Service–Curve Number (SCS-CN) method for estimation of losses incorporating the relationship between soil saturation and the parameter  $S$  (soil potential maximum retention) of the SCS-CN method as proposed by [Brocca et al. \(2009\)](#). Three different components contribute to generate discharge: the surface runoff, the saturation excess and the subsurface runoff component. The first two are summed and routed to the outlet by the Geomorphological Instantaneous Unit Hydrograph (GIUH). The subsurface runoff is transferred to the outlet section by a linear reservoir approach. For both routing schemes, the lag time is evaluated by the

relationship proposed by [Melone et al. \(2002\)](#). Full details on model equations are already given in [Brocca et al. \(2009; 2011\)](#) and, hence, are not repeated here. The MATLAB® code of the model is freely available at: <http://hydrology.irpi.cnr.it/people/l.brocca>.

MISDc uses 8 parameters, i.e., the maximum soil water capacity, the pore size distribution index, the saturated hydraulic conductivity, the fraction of percolated water that generates baseflow, the lag-area relationship coefficient, a correction parameter for the evapotranspiration, the initial abstraction coefficient of the SCS-CN method and the coefficient of the relationship relating SM to the initial condition of the SCS-CN method. As input data, the model needs continuous rainfall and temperature timeseries. The calibration step is carried out in MATLAB® environment by using a standard gradient-based automatic optimization method ([Bober, 2013](#)) and the maximization of the Nash-Sutcliffe efficiency index is considered as objective function.

## 2.4 Performance metrics

The assessment of the model performances, driven by ground rainfall observations and SRPs, is carried out in terms of Nash-Sutcliffe efficiency ( $NS$ ), correlation coefficient ( $R$ ) and percentage volume error ( $E_v$ ).  $NS$  is often used for hydrological modelling assessment and it ranges between  $-\infty$  and 1. The closer the index is to 1, the better the performance is.  $NS$  index is defined as:

$$NS = 1 - \frac{\sum_{t=1}^n (Q_{obs} - Q_{sim})^2}{\sum_{t=1}^n (Q_{obs} - \overline{Q_{obs}})^2} \quad (6)$$

where  $Q_{obs}$  and  $Q_{sim}$  are the observed and simulated discharge at time  $t$ , while  $\overline{Q_{obs}}$  is the temporal mean of observed discharge.

The percentage volume errors,  $E_v$ , is expressed by the following equation:

1  
2  
3  
4  
5  
6  
7  
8  
9  
10  
11  
12  
13  
14  
15  
16  
17  
18  
19  
20  
21  
22  
23  
24  
25  
26  
27  
28  
29  
30  
31  
32  
33  
34  
35  
36  
37  
38  
39  
40  
41  
42  
43  
44  
45  
46  
47  
48  
49  
50  
51  
52  
53  
54  
55  
56  
57  
58  
59  
60  
61  
62  
63  
64  
65

$$E_v = \frac{\sum_{t=1}^n Q_{obs} - \sum_{t=1}^n Q_{sim}}{\sum_{t=1}^n Q_{obs}} 100 \quad (7)$$

Positive  $E_v$  values indicate discharge underestimation while negative ones, an overestimation. The performance metrics are calculated during both the calibration and validation period, for each rainfall input dataset.

For each basin, the most significant flood events are extracted in order to assess the capability of the considered rainfall datasets in reproducing the flood hydrograph, volume and peak at the event-scale. The evaluation is carried out by considering the indexes described above, computed for each flood event, and by using the percentage error in peak discharge, expressed by the following equation:

$$E_{Qp} = \frac{\max(Q_{obs}) - \max(Q_{sim})}{\max(Q_{obs})} \quad (8)$$

A negative error highlights overestimation, while a positive value means underestimation.

### 3. RESULTS AND DISCUSSIONS

The hydrological validation of satellite rainfall datasets is described for both the calibration and the validation period, for each of the 5 rainfall datasets, and over the 4 selected basins considered in the study.

#### 3.1 Rainfall datasets comparison

First, an intercomparison of rainfall datasets is carried out in order to evaluate the quality of input data used to drive MISDc model. This analysis is carried out by considering  $R$  and the root mean square error ( $RMSE$ ) between the daily ground and the satellite mean areal rainfall during the calibration and the validation periods. Results, reported in *Table 2*, show a satisfactorily agreement

1  
2  
3  
4  
5  
6  
7  
8  
9  
10  
11  
12  
13  
14  
15  
16  
17  
18  
19  
20  
21  
22  
23  
24  
25  
26  
27  
28  
29  
30  
31  
32  
33  
34  
35  
36  
37  
38  
39  
40  
41  
42  
43  
44  
45  
46  
47  
48  
49  
50  
51  
52  
53  
54  
55  
56  
57  
58  
59  
60  
61  
62  
63  
64  
65

between the ground and satellite derived rainfall datasets. SM2R<sub>ASC</sub> provides lower performance scores than TMPA: this is probably due to the algorithm calibration procedure, based on 5 days of accumulated rainfall ([Ciabatta et al., 2015b](#)). All the analysed datasets provide  $R$  values higher than 0.48 and quite low  $RMSE$  values. The higher  $RMSE$  values over Brenta basin are due to the high rainfall regime and the presence of mountains that might affect the satellite retrievals accuracy. The obtained results are in line with those showed by [Ciabatta et al. \(2015b\)](#) who obtained median  $R$  values over the Italian territory equal to 0.44 and 0.59 for SM2R<sub>ASC</sub> and TMPA, respectively, for 1 day of accumulated rainfall. Moreover, similar results are also obtained by [Stampoulis and Anagnostou \(2011\)](#) and [Nikolopoulos et al. \(2013\)](#) who evaluated the real-time TMPA product over Northern Italy.

### 3.2 Discharge simulation with ground observed rainfall

The performance scores obtained by forcing MISDc model with OBS are assessed in order to evaluate the model capability in reproducing observed discharges and are used as benchmark to highlight any increase (or deterioration) in model accuracy when using SRPs.

*Figure 3* shows the simulated discharge timeseries obtained by forcing MISDc with OBS data. As it can be seen, the model is able to reproduce the observed discharge well, showing  $NS$  values of 0.72, 0.76, 0.77 and 0.86 during the calibration period (2010-2011) for Brenta, Tanaro, Tiber and Volturno basins, respectively. During the validation period (2012-2013), the simulations provide  $NS$  values of 0.76, 0.68, 0.52 and 0.77 with only a slight deterioration of model performance. In terms of correlation, the model provides  $R$  values greater than 0.86 (0.77) during the calibration (validation) period. For what concerns the errors in volume, MISDc simulations provide  $E_v$  values lower than 23% in calibration and lower than 15% during the validation step. These not negligible errors in volume are partly due to the difficulties of the model in reproducing the low flows and to the objective function used for model calibration (maximization of  $NS$ ) that is mainly addressed for the reproduction of high

1  
2  
3  
4  
5  
6  
7  
8  
9  
10  
11  
12  
13  
14  
15  
16  
17  
18  
19  
20  
21  
22  
23  
24  
25  
26  
27  
28  
29  
30  
31  
32  
33  
34  
35  
36  
37  
38  
39  
40  
41  
42  
43  
44  
45  
46  
47  
48  
49  
50  
51  
52  
53  
54  
55  
56  
57  
58  
59  
60  
61  
62  
63  
64  
65

flows. In addition, as it can be noticed by *Figure 3*, some discharge peaks are not correctly identified, as over Brenta basin during the calibration period and over Tanaro in 2011. These errors might be due to different causes, for example the inaccuracy of input observations and the modelling structure, to the effect of spatial variability that is neglected here, and to the daily time step used for the simulation that could be not fully appropriate for fast responding basins. Despite these limitations, MISDc confirms its good capability in simulating floods, also in different physiographic and climatic conditions in Italy, thus representing an useful tool for testing the potential added-value of SRPs for flood forecasting. All the performance scores obtained with each rainfall product, for the calibration and validation period, are summarized in *Table 3*.

**3.3 Discharge simulation with satellite rainfall products**

Before introducing the bias correction and recalibration steps into the workflow, discharge simulations are carried out by using the raw SRPs. By way of example, *Figure 4* shows the observed and simulated hydrographs for Tanaro basin obtained by forcing MISDc with TMPA rainfall dataset without and with the application of the bias correction step. As it can be seen, if the model is forced with bias corrected data and after the recalibration, higher performances are obtained. Indeed, the obtained performance scores, before and after the bias correction and the model recalibration, increase from  $NS=0.40$ ,  $R=0.71$  and  $E_v=35\%$ , to  $NS=0.53$ ,  $R=0.77$  and  $E_v=9\%$ . Although the improvement is not so significant, the effect of the two pre-processing steps is evident. In most of the cases (results not shown for brevity) the simulations carried out by using corrected data provide higher performance scores than those obtained by using the raw data. Exceptions are found for the Brenta and Tanaro during the validation period for TMPA and for Brenta and Volturno during the calibration period for SM2R<sub>ASC</sub>. These results may be due to the high variability of the rainfall regime from year to year which would need a dynamic correction of the bias or its more frequent recalibration. On this basis, the

1  
2  
3  
286  
5  
6  
287  
8  
288  
10  
11  
289  
12  
13  
290  
15  
16  
291  
17  
18  
292  
20  
293  
22  
23  
294  
24  
25  
295  
27  
28  
296  
29  
30  
297  
32  
33  
298  
34  
35  
299  
37  
38  
300  
39  
40  
301  
42  
302  
44  
45  
303  
46  
47  
304  
49  
50  
305  
51  
52  
306  
54  
55  
307  
56  
57  
308  
59  
60  
61  
62  
63  
64  
65

correction of the bias is in general beneficial but may also provide additional uncertainties in case the rainfall presents a high non-stationary character. Moreover, it is obtained that after the recalibration, all the parameter values remained into a physically acceptable range of variation thus ensuring the consistency of the hydrological simulations. The small but consistent improvement in hydrological model performance after bias correction of TMPA product (and model recalibration) is also obtained by [Artan et al. \(2007\)](#) for two sub-basins of Mekong River in South Asia, [Stisen and Sandhot \(2010\)](#) for the Senegal River basin in West Africa, [Tarnavsky et al. \(2013\)](#) in Senegal and Tunisia, and [Zhao et al. \(2015\)](#) in the Weihe River basin in China. Therefore, due to the overall improved performances, in the following we show only results in which SRPs bias is corrected through ground observations and the model parameter values are recalibrated for each SRP (in the calibration period).

The comparison between observed and simulated discharge obtained by using TMPA and SM2R<sub>ASC</sub> as input is reported in *Figure 5*. Although a general agreement between observed and simulated discharge is recognizable, some peaks are not identified (mainly in the Brenta basin) or overestimated (Tanaro and Tiber basins) likely due to errors in the SRPs used here as input data.

More specifically, when SM2R<sub>ASC</sub> is used as input, a deterioration of the results with respect to those obtained by using OBS is found, with *NS* values of 0.63 (0.52) for Brenta, 0.60 (0.48) for Tanaro, 0.66 (0.48) for Tiber and 0.63 (0.48) for Volturno during the period 2010-2011 (2012-2013). The lower scores are probably due to SM2RAIN algorithm limitations, i.e., underestimation of rainfall when the soil is close to saturation and to the presence of mountains and/or snow within the basin that affects the SM data quality (and, hence, of the SM2RAIN-derived rainfall). The first issue can be easily observed over the Tiber basin at the end of 2012, when a discharge peak of over 500 m<sup>3</sup>/s is not identified. The latter issue is evident over Brenta and Tanaro basins characterized by higher uncertainty in SM data and a general underestimation of river discharge. In terms of correlation coefficient, SM2R<sub>ASC</sub> still

1  
2  
3  
309  
5  
310  
6  
8  
311  
10  
312  
11  
12  
13  
313  
15  
314  
17  
315  
20  
316  
22  
317  
24  
25  
318  
27  
319  
29  
30  
320  
32  
321  
34  
35  
322  
37  
323  
39  
40  
324  
42  
325  
44  
326  
45  
47  
327  
49  
328  
50  
51  
52  
329  
54  
330  
55  
56  
57  
331  
58  
59  
60  
61  
62  
63  
64  
65

provides fair  $R$  values for all the analysed basins: during the calibration (validation) period  $R$  values greater than 0.73 (0.70) are obtained for the analysed basins. In terms of errors in volume, quite low  $E_v$  values are observed during the calibration (validation) period: -2% (-4%) for Brenta, 13% (10%) for Tanaro, 3% (-1%) for Tiber and -3% (-32%) for Volturno. The negative values, mainly obtained during the last two years of the analysis period, highlight an overestimation of discharge.

When MISDc is forced with TMPA, lower  $NS$  values are obtained, even negative during the validation period.  $R$  values are greater than 0.60 (0.36) during the calibration (validation) period and an overall discharge underestimation is observed with  $E_v$  values lower than 6% and 36% in the calibration and validation period, respectively. It is likely that the lower performance scores are due to the accuracy of the TMPA product, which is highly affected by topographic issue and by the type and intensity of precipitation. Indeed, [Ciabatta et al. \(2015b\)](#) highlighted that TMPA product shows low performance in Southern Italy and in areas characterized by an intense rainfall regime (e.g., Brenta basin). Moreover, the low and even negative scores obtained during the validation period are likely due to the need of a more frequent correction of the bias in order to take into account its variability due also to the changes in the retrieval algorithms and measurement sensors (note that the TMPA product is based on measurements from a constellation of satellite sensors that are changing in time). A monthly analysis (not shown) was also carried out in order to investigate the reasons of the low performance of MISDc using TMPA during the validation period and by analysing both rainfall and discharge data. The analysis has shown that the performance in terms of rainfall reproduction (by using ground observations as benchmark) of TMPA during the validation period are highly variable (much more than in the calibration period), with some months in which the performance reaches very low values (e.g.,  $R < 0.2$ ). Therefore, it appears that any error or performance reduction in rainfall estimation have a significant impact on the hydrological simulation and propagates forward in time for several months.



1  
2  
3  
332  
5  
6  
333  
7  
8  
334  
10  
11  
335  
12  
13  
336  
15  
16  
337  
17  
18  
338  
20  
21  
339  
22  
23  
340  
24  
25  
341  
27  
28  
342  
29  
30  
343  
32  
33  
344  
34  
35  
36  
345  
38  
39  
346  
40  
41  
347  
43  
44  
348  
45  
46  
349  
48  
49  
350  
50  
51  
351  
52  
53  
352  
55  
56  
353  
57  
58  
354  
60  
61  
62  
63  
64  
65

As a result, any short period in which rainfall estimates are less accurate produces remarkable errors in the simulation of discharge and it is the main reason for the observed low performance of TMPA in the validation period.

In Italy, just a work by [Nikolopoulos et al. \(2013\)](#) evaluated the reliability of different SRPs for discharge simulation but their study was addressed to the simulation of only a limited number of flood events and not a continuous simulation such as we have performed here. The obtained performances are in agreement anyhow with those obtained by previous studies in different regions worldwide ([Artan et al., 2007](#); [Stisen and Sandhot, 2010](#); [Zhao et al., 2015](#)). We note also that the discharge simulation in Mediterranean areas is more complex than that one for large basins in Africa or South Asia that are characterized by a consistent and pronounced seasonal cycle and that are the basins in which most of the studies were carried out by employing SRPs (see [Serrat-Capdevilla et al., 2013](#) for a review). Therefore, the results obtained here highlight that SRPs may be employed with some skill also in smaller basins of the Mediterranean region.

### 3.4 Discharge simulation by using the integrated rainfall datasets

The integration procedure between ground observed and satellite rainfall by using *Equation (3)* provides improvements in the performance scores, showing *NS* values most of the times (for 3 out 4 basins) higher than those obtained by using observed rainfall, mainly for SM2R<sub>ASC</sub>+OBS product (see bold numbers in *Table 3*). *Table 4* reports *K* values obtained during the calibration period for each rainfall dataset. The simple integration scheme here proposed involves very high values of *K*, except for TMPA+OBS in the Tanaro basin that shows the lowest *K* value equal to 0.5. It should be noted that the high weight given to ground observations is expected due the high quality of ground observed rainfall datasets used in this analysis. As it can be noticed in *Figure 6*, the use of the integrated datasets into MISDc allows to obtain an accurate discharge simulation over the four analysed basins. It is worth

1  
2  
3  
4  
5 to notice that some of the discharge peaks are still not properly identified by the simulated discharge.  
6  
7 This is not due to the SRPs quality, as the same events are also not well captured in the simulations  
8  
9 carried out by using OBS as input (see *Figure 3*). Therefore, these errors have to be attributed to the  
10  
11 reasons highlighted in Section 3.2 and specifically to the MISDc model deficiencies in representing the  
12  
13 hydrological behaviour of the basins throughout the year.  
14

15  
16 The integration between observed and satellite rainfall improves the model performance for all the  
17  
18 basins except Volturno basin. *Figure 7* shows the mostly positive percentage variations of *NS* values  
19  
20 obtained by using OBS and the integrated products over the four basins, both during the calibration and  
21  
22 validation period. During calibration, SM2RASC+OBS (TMPA+OBS) provides *NS* values greater than  
23  
24 0.77 (0.75), while during validation *NS* values greater than 0.63 (0.36) are obtained. In terms of  
25  
26 correlation, similar results are obtained. That is, SM2R<sub>ASC</sub>+OBS provides *R* values higher than 0.88  
27  
28 and 0.82 during calibration and validation, respectively, while TMPA+OBS dataset yields *R* higher  
29  
30 than 0.87 and 0.73. The use of integrated rainfall datasets provides also a reduction of the error in  
31  
32 volume, for all basins.  
33  
34  
35  
36  
37  
38

### 39 **3.5 Model performance for flood events**

40  
41 The analysis of the performance has been carried out on a total of 43 flood events extracted from  
42  
43 the analysed timeseries: 11 for Tanaro basin, 12 for Brenta basin, 10 for Tiber and Volturno basins. The  
44  
45 events were extracted by selecting those characterized by a total rainfall of more than 20 mm. An event  
46  
47 is distinguished from another if a total rainfall less than 1 mm occurred for at least 6 h. Specifically, the  
48  
49 performance are assessed by considering the hydrographs obtained by forcing MISDc with the different  
50  
51 rainfall datasets, and thus, no recalibration based on flood events is carried out. In *Figure 8* the  
52  
53 performance scores obtained for each flood event and basin are shown. It can be noticed that if MISDc  
54  
55 is forced with OBS data, quite high *NS* values are obtained, except for Tiber basin which is  
56  
57  
58  
59  
60  
61  
62  
63  
64  
65

1  
2  
3  
4  
5  
6  
7  
8  
9  
10  
11  
12  
13  
14  
15  
16  
17  
18  
19  
20  
21  
22  
23  
24  
25  
26  
27  
28  
29  
30  
31  
32  
33  
34  
35  
36  
37  
38  
39  
40  
41  
42  
43  
44  
45  
46  
47  
48  
49  
50  
51  
52  
53  
54  
55  
56  
57  
58  
59  
60  
61  
62  
63  
64  
65

characterized by lower performance scores. These results are in agreement with those obtained by [Brocca et al. \(2011b\)](#) in Central Italy and by [Massari et al. \(2015\)](#) throughout the Italian territory who obtained  $NS$  values at the event-scale ranging between 0.50 and 0.95. If TMPA and SM2R<sub>ASC</sub> datasets are used as input data, lower performance can be observed with an average reduction of  $NS$  equal to -40% and -36% for TMPA and SM2R<sub>ASC</sub>, respectively. More in details, TMPA provides the worst performance with several negative  $NS$  values over Tanaro and Brenta basins (e.g., event 8 for Tanaro and event 11 for Brenta). SM2R<sub>ASC</sub> provides  $NS$  values comparable with those obtained by forcing MISDc with OBS over Tanaro, Brenta and Tiber basins, while  $NS$  is consistently lower for Volturno basin. The integrated products provide results comparable and sometimes higher than those obtained by using OBS, except for event 8 over Tanaro basin, where TMPA+OBS product yields a  $NS$  value of about -2.

In terms of  $E_{Op}$ , a general underestimation of peak discharge can be observed by using OBS as input data. Even in this case, the simulations over Tiber basin provide the worst performance scores, with an error of about 50% for events 3, 4, 6, 7, 8 and 9 and about -100% for event 7. TMPA product provides a general underestimation of the discharge peaks over Tanaro, Brenta and Tiber basins. SM2R<sub>ASC</sub> is characterized by a general underestimation over all the four analysed basins, mainly for Tiber and Volturno basins. TMPA+OBS and SM2R<sub>ASC</sub>+OBS products provide  $E_{Op}$  values similar to those obtained if MISDc is driven with OBS and even lower error values (with respect to OBS) over Brenta basin. In terms of  $E_v$ , OBS data provide the best performance scores, mainly for Volturno basin. TMPA and SM2R<sub>ASC</sub> products are characterized by a general underestimation for Tanaro, Brenta and Tiber basins while the simulations carried out for Volturno basin provide better results with respect to the other basins, except for event 10.

1  
2  
3  
400 To sum up, in terms of median  $NS$  on all the selected flood events, the use of integrated products  
5  
6  
401 provides comparable results with those achieved by using OBS with the best performance obtained for  
7  
8  
402 Tiber River for  $SM2R_{ASC}+OBS$  (+54%) and Brenta basin by using  $TMPA+OBS$  (+14%) and worst  
9  
10  
403 ones obtained for Volturno with  $TMPA+OBS$  (-18%). In the remainder of the cases both  
11  
12  
404  $SM2R_{ASC}+OBS$  and  $TMPA+OBS$  yields values close to OBS with better results obtained by  
13  
14  
405  $SM2R_{ASC}+OBS$ . The poor results obtained for Volturno basin can be explained by the relatively high  
15  
16  
406 quality OBS data when they are used as input in MISDc. Similar results are obtained for  $E_{Op}$  ( $E_v$ ) with  
17  
18  
407 an error reduction of about 28% (38%) for Tiber basin by using  $SM2R_{ASC}+OBS$  and 43% (16%) for  
19  
20  
408 Brenta basin by using  $TMPA+OBS$ .

21  
22  
409 If compared with the study by [Massari et al. \(2014\)](#), who forced a rainfall-runoff model over a  
23  
24  
410 small catchment in France by using an estimated rainfall product obtained by the application of  
25  
26  
411  $SM2RAIN$  to in situ SM observations, a good agreement in the obtained results is observed. Indeed,  
27  
28  
412 [Massari et al. \(2014\)](#) found that the use of the  $SM2RAIN$ -derived rainfall provides reasonable results  
29  
30  
413 but lower than using traditional raingauge observations. However, accordingly our study, the  
31  
32  
414 integration of observed (from raingauge) and estimated rainfall (from  $SM2RAIN$ ) provided the best  
33  
34  
415 performance with an increase in the mean  $NS$  equal to 38% (from 0.48 to 0.66).  
35  
36  
37  
38  
39  
40  
41  
42  
43  
44

#### 416 **4. CONCLUSIONS**

417 Daily discharge simulation with the lumped MISDc model is carried out over four basins  
418 throughout the Italian territory and by using ground observed and satellite-derived rainfall data. The  
419 analysis produced satisfactory and promising results and highlighted the beneficial effects of using  
420 satellite rainfall products in flood modelling over the four analysed basins. Concerning the obtained  
421 results, the following conclusions can be drawn:  
422  
423  
424  
425  
426  
427  
428  
429  
430  
431  
432  
433  
434  
435

- MISDc hydrologic model is able to reproduce accurately discharges over 4 basins, characterized by different physiographic and climatic conditions, especially in high flow conditions. MISDc simulations forced by ground observed rainfall provide Nash-Sutcliffe efficiency values greater than 0.72 and 0.52 during the calibration and validation period (*Table 3* and *Figure 3*);
- Satellite rainfall products can be employed for flood simulation, but bias correction and model parameters recalibration are needed before their use (*Figure 4*). The simulations have provided promising results in terms of Nash Sutcliffe efficiency, correlation coefficient and volume error, mainly during the calibration period (*Table 3*). However, this analysis has highlighted some contrasting results (as the negative *NS* values for TMPA in the validation period) that have to be assessed in further studies by analysing a longer period and by taking into account the year-to-year variability of rainfall regimes;
- SM2R<sub>ASC</sub> performances confirm the good capability of SM2RAIN algorithm in estimating rainfall, allowing to apply successfully the method also for flood simulation. If MISDc is driven by SM2R<sub>ASC</sub> data, even better performance scores than TMPA product are obtained (*Figure 5*);
- Ground observed rainfall datasets may be affected by spatial representativeness issues and may lead to wrong discharge simulations: the simple integration scheme proposed in this study highlights the capability of satellite rainfall products to improve rainfall estimates. Although the improvements are not so evident, MISDc simulations driven by SM2R<sub>ASC</sub>+OBS and TMPA+OBS provide performance scores, in most of the cases (3 out 4 basins), better than those obtained by using only the ground observed data. We expect that more advanced integration schemes may help to further enhance the results.

1  
2  
3  
4  
445 Notwithstanding the obtained results are related to the availability and reliability of ground  
5  
6  
446 observed data, this study provides promising results and represents one of the first attempts to integrate  
7  
8  
447 ground observed and satellite rainfall datasets for flood simulation, mainly in well gauged areas. More  
9  
10  
11  
448 detailed analysis will be addressed in the future in order to better understand and improve the capability  
12  
13  
449 of SRPs in hydrological modelling, by using different bias correction formulations, a more  
14  
15  
450 sophisticated integrations scheme (e.g., data assimilations technique) and by selecting a larger number  
16  
17  
451 of study basins worldwide. The integration between SRPs without the use of ground observed rainfall  
18  
19  
20  
452 data will be analysed as well.  
21  
22  
23  
24  
25

## 453 **ACKNOWLEDGEMENTS**

26  
454 The Italian Civil Protection Department is gratefully acknowledged for providing the observed  
27  
28  
29  
30  
455 data from the Italian monitoring network. Funding by EUMESAT through the “Satellite Application  
31  
32  
33  
456 Facility on Support to Operational Hydrology and Water Management (H-SAF)” project is also  
34  
35  
457 gratefully acknowledged.  
36  
37  
38  
39

## 458 **REFERENCES**

- 40  
41  
42  
459 Artan, G., Gadain, H., Smith, J.L., Asante, K., Bandaragoda, J., Verdin, J.P. (2007). Adequacy of  
43  
44  
45  
460 satellite derived rainfall data for stream flow modeling. *Nat. Hazards*, 43, 167-185.  
46  
47  
48  
461 Bober, W. (2013). *Introduction to Numerical and Analytical Methods with MATLAB for Engineers  
49  
50  
51  
462 and Scientists*. CRC Press, Inc.: Boca Raton, FL, USA.  
52  
53  
463 Brocca, L., Melone, F., Moramarco, T. (2008). On the estimation of antecedent wetness conditions in  
54  
55  
56  
464 rainfall-runoff modelling. *Hydrological Processes*, 22 (5), 629-642.  
57  
58  
59  
465 Brocca, L., Melone, F., Moramarco, T., Singh, V.P. (2009). A continuous rainfall –runoff model as a  
60  
61  
62  
466 tool for the critical hydrological scenario assessment in natural channels. In: M. Taniguchi, W.C.  
63  
64  
65  
467 Burnett, Y. Fukushima, M. Haigh, Y. Umezawa (Eds), *From headwater to the ocean.*  
468  
Hydrological changes and managements, Taylor & Francis Group, London, 175-179.

1  
2  
3  
4  
5  
6  
7  
8  
9  
10  
11  
12  
13  
14  
15  
16  
17  
18  
19  
20  
21  
22  
23  
24  
25  
26  
27  
28  
29  
30  
31  
32  
33  
34  
35  
36  
37  
38  
39  
40  
41  
42  
43  
44  
45  
46  
47  
48  
49  
50  
51  
52  
53  
54  
55  
56  
57  
58  
59  
60  
61  
62  
63  
64  
65

469 Brocca L., Hasenauer, S., Lacava, T., Melone, F., Moramarco, T., Wagner, W., Dorigo, W., Matgen,  
470 P., Martinez.Fernandez, J., Llorens, P., Latron, J., Martin, C., Bittelli, M. (2011a). Soil moisture  
471 estimation through ASCAT and AMSR-E sensors: an intercomparison and validation study  
472 across Europe. *Remote Sensing of Environment*, 115, 3390-3408.

473 Brocca, L., Melone, F., Moramarco, T. (2011b). Distributed rainfall-runoff modelling for flood  
474 frequency estimation and flood forecasting. *Hydrological Processes*, 25 (18), 2801-2813.

475 Brocca, L., Liersch, S., Melone, F., Moramarco, T., Volk, M. (2013a). Application of a model-based  
476 rainfall-runoff database as efficient tool for flood risk management. *Hydrology and Earth System  
477 Sciences*, 17, 3159-3169.

478 Brocca, L., Melone, F., Moramarco, T., Wagner, W. (2013b). A new method for rainfall estimation  
479 through soil moisture observations. *Geophys. Res. Lett.*, 40(5), 853-858.

480 Brocca, L., Ciabatta, L., Massari, C., Moramarco, T., Hahn, S., Hasenauer, S., Kidd, R., Dorigo, W.,  
481 Wagner, W., Levizzani, V. (2014). Soil as a natural raingauge: estimating rainfall from global  
482 satellite soil moisture data. *J. Geophys. Res.*, 119(9), 5128–5141.

483 Ciabatta, L., Brocca, L., Moramarco T., Wagner, W. (2015a). Comparison of different satellite rainfall  
484 products over the Italian territory. Conference proceeding of XII International IAEG congress,  
485 Torino, 15-19 September. *Engineering Geology For Society And Territory - Volume 3*, 978-3-  
486 319-09053-5, 326570\_1\_En (126).

487 Ciabatta, L., Brocca, L., Massari, C., Moramarco, T., Puca, S., Rinollo, A., Gabellani, S., Wagner, W.  
488 (2015b). Integration of soil moisture and rainfall observations over the Italian territory. *Journal of  
489 Hydrometeorology*, 16(3), 1341-1355.

490 Dee, D.P., et al. (2011). The ERA-Interim reanalysis: Configuration and performance of the data  
491 assimilation system. *Quart. J. Roy. Meteor. Soc.*, 137, 553-597.

492 Doorenbos J, Pruitt WO. 1977. Background and development of methods to predict reference crop  
493 evapotranspiration (ET<sub>o</sub>). In *Crop Water Requirements*. FAO Irrigation and Drainage Paper No.  
494 24, FAO: Rome; 108–119 (Appendix II).

495 Draper, C., Walker, J. P., Steinle, P., De Jeu, R. A. M., & Holmes, T. R. H. (2009). An evaluation of  
496 AMSR-E derived soil moisture over Australia. *Remote Sensing of Environment*, 113(4), 703–710

497 Famiglietti JS, Wood EF. (1994). Multiscale modeling of spatially variable water and energy balance  
498 processes. *Water Resources Research*, 11, 306-3078.

499 Guetter, A.K, Georgakakos, K.P., Tsonis, A.A. (1996). Hydrologic applications of satellite data: 2.  
500 Flow simulation and water estimates. *Journal of Geophysical Research*, 101, 26527-26538.

501 Harris, A., Rahman, S., Hossain, F., Yarborough, L., Bagtzoglou, A.C., Easson, G. (2007). Satellite-  
502 based flood modeling using TRMM-based rainfall products. *Sensors*, 7, 3416-3427.

1  
2  
3  
503  
504  
505  
8  
506  
507  
11  
508  
509  
510  
16  
511  
512  
513  
21  
514  
515  
516  
25  
517  
518  
29  
519  
520  
521  
33  
522  
523  
524  
38  
525  
526  
527  
43  
528  
529  
530  
48  
531  
532  
51  
533  
534  
535  
536  
57  
58  
59  
60  
61  
62  
63  
64  
65

Hou, A.Y., Kakar, R.K., Neeck, S., Azarbarzin, A.A., Kummerow, C.D., Kojima, M., Oki, R., Nakamura, K., Iguchi, T. (2013). The Global Precipitation Measurement (GPM) mission. *Bull. Amer. Meteor. Soc.*, 95(5), 701-722.

Hsu KL, Gao XG, Sorooshian S, Gupta HV. 1997. Precipitation estimation from remotely sensed information using artificial neural networks. *Journal of Applied Meteorology*, 36(9), 1176-1190.

Huffman, G.J., R.F. Adler, D.T. Bolvin, G. Gu, E.J. Nelkin, K.P. Bowman, Y. Hong, E.F. Stocker, D.B. Wolff, 2007. The TRMM Multi-satellite Precipitation Analysis: Quasi-Global, Multi-Year, Combined-Sensor Precipitation Estimates at Fine Scale. *J. Hydrometeorol.*, 8(1), 38-55.

Jongman, B., Hochrainer-Stigler, S., Feyen, L., Aerts, J.C., Mechler, R., Botzen, W.W., Bouwer, L.M., Pflug, G., Rojas, R., Ward, P.J. (2014). Increasing stress on disaster-risk finance due to large floods. *Nature Climate Change*, 4(4), 264-268.

Joyce RJ, Janowiak JE, Arkin PA, Xie PP. 2004. CMORPH: A method that produces global precipitation estimates from passive microwave and infrared data at high spatial and temporal resolution. *Journal of Hydrometeorology*, 5(3), 487-503.

Kidd, C., V. Levizzani, 2011. Status of satellite precipitation retrievals. *Hydrol. Earth Syst. Sci.*, 15, 1109-1116.

Kidd, C., P. Bauer, J. Turk, G.J. Huffman, R. Joyce, K.L. Hsu, D. Braithwaite, 2012. Intercomparison of high-resolution precipitation products over the northwest Europe. *J. Hydrometeorol.*, 13, 67-83.

Kucera, P.A., E.E. Ebert, F.J. Turk, V. Levizzani, D. Kirschbaum, F.J. Tapiador, A. Loew, M. Borsche, 2013. Precipitation from space: Advancing earth system science. *Bull. Amer. Meteor. Soc.*, 94, 365-375.

Massari, C., L. Brocca, T. Moramarco, Y. Trambly, J-F. Didon Lescot. (2014). Potential of soil moisture observations in flood modelling: estimating initial conditions and correcting rainfall. *Adv. Water Resour.*, 74, 44-53.

Massari, C., Brocca, L., Ciabatta, L., Moramarco, T., Gabellani, S., Albergel, C., De Rosnay, P., Puca, S., Wagner, W. (2015). The use of H-SAF soil moisture products for operational hydrology: flood modelling over Italy. *Hydrology*, 2, 2-22.

Melone, F., Corradini, C., Singh, V.P. (2002). Lag prediction in ungauged basins: an investigation through actual data of the upper Tiber River valley. *Hydrological Processes*, 16, 1085-1094.

Mugnai, A., Casella, D., Cattani, E., Dietrich, S., Laviola, S., Levizzani, V., Panegrossi, G., Petracca, M., Sanò, P., Di Paola, F., Biron, D., De Leonibus, L., Melfi, D., Rosci, P., Vocino, A., Zauli, F., Pagliara, P., Puca, S., Rinollo, A., Milani, L., Porcù, F., Gattari, F. (2013). Precipitation products from the hydrology SAF, *Nat. Hazards Earth Syst. Sci.*, 13, 1959-1981.



1  
2  
3  
537  
538  
539  
8  
540  
541  
542  
12  
13  
543  
544  
545  
17  
546  
19  
20  
21  
548  
549  
24  
550  
26  
27  
28  
552  
30  
553  
32  
33  
34  
35  
556  
557  
38  
558  
39  
40  
560  
42  
561  
44  
562  
46  
563  
47  
48  
564  
565  
566  
52  
53  
54  
55  
56  
57  
58  
59  
60  
61  
62  
63  
64  
65

Nikolopoulos, E.I., Anagnostou, E.N., Borga, M. (2013). Using high-resolution satellite rainfall products to simulate a major flash flood event in northern Italy. *Journal of Hydrometeorology*, 14(1), 171-185.

Rudolf, B. and U. Schneider, 2005. Calculation of gridded precipitation data for the global land-surface using in-situ gauge observations. *Proc. 2nd Workshop Int. Precipitation Working Group, 2005*, 231-247.

Serrat-Capdevilla, A., Valdes, J.B., Stakhiw, E.Z. (2013). Water management applications for satellite precipitation products: synthesis and recommendations. *Journal of the American Water Resources Association (JAWRA)*, 50(2), 509-525.

Stampoulis, D., Anagnostou, E.N. (2011). Evaluation of global satellite rainfall products over continental Europe. *J. Hydrometeor.*, 13, 588–603.

Stisen, S., Sandholt, I. (2010). Evaluation of remote-sensing-based rainfall products through predictive capability in hydrological runoff modelling. *Hydrological Processes*, 24, 879-891.

Tarnavsky, E., Mulligan, M., Ouessar, M., Faye, A., Black, E. (2013). Dynamic Hydrological Modeling in Drylands with TRMM Based Rainfall. *Remote Sensing*, 5(12), 6691-6716.

The NOAA Climate Prediction Center, N., 2002. African Rainfall Estimation Algorithm – Version 2.0.

Thieming, V., Rojas, R., Zambrano-Bigiarini, M., De Roo, A. (2013). Hydrological evaluation of satellite-based rainfall estimates over the Volta and Baro-Akobo Basin. *Journal of Hydrology*, 499, 324-338.

Wagner, W., Hahn, S., Kidd, R., Melzer, T., Bartalis, Z., Hasenauer, S., Figa, J., de Rosnay, P., Jann, A., Schneider, S., Komma, J., Kubu, G., Brugger, K., Aubrecht, C., Zuger, J., Gangkofner, U., Kienberger, S., Brocca, L., Wang, Y., Bloeschl, G., Eitzinger, J., Steinnocher, K., Zeil, P., Rubel, F. (2013). The ASCAT Soil Moisture Product: A Review of its Specifications, Validation Results, and Emerging Applications. *Meteorologische Zeitschrift*, 22(1), 5-33.

Wake B. (2013). Flooding costs. *Nature Climate Change*, 3, 778.

Xie P, Arkin AP (1997) Global precipitation: a 17-year monthly analysis based on gauge observations, satellite estimates, and numerical model outputs. *Bull Am Meteorol Soc*, 78(11), 2539-2558.

Zhao, H., Yang, S., Wang, Z., Zhou, X., Luo, Y., Wu, L. (2015). Evaluating the suitability of TRMM satellite rainfall data for hydrological simulation using a distributed hydrological model in the Weihe River catchment in China. *Journal of Geographical Sciences*, 25(2), 177-195.

1  
2  
3  
4  
5  
6  
7  
8  
9  
10  
11  
12  
13  
14  
15  
16  
17  
18  
19  
20  
21  
22  
23  
24  
25  
26  
27  
28  
29  
30  
31  
32  
33  
34  
35  
36  
37  
38  
39  
40  
41  
42  
43  
44  
45  
46  
47  
48  
49  
50  
51  
52  
53  
54  
55  
56  
57  
58  
59  
60  
61  
62  
63  
64  
65

**FIGURES**

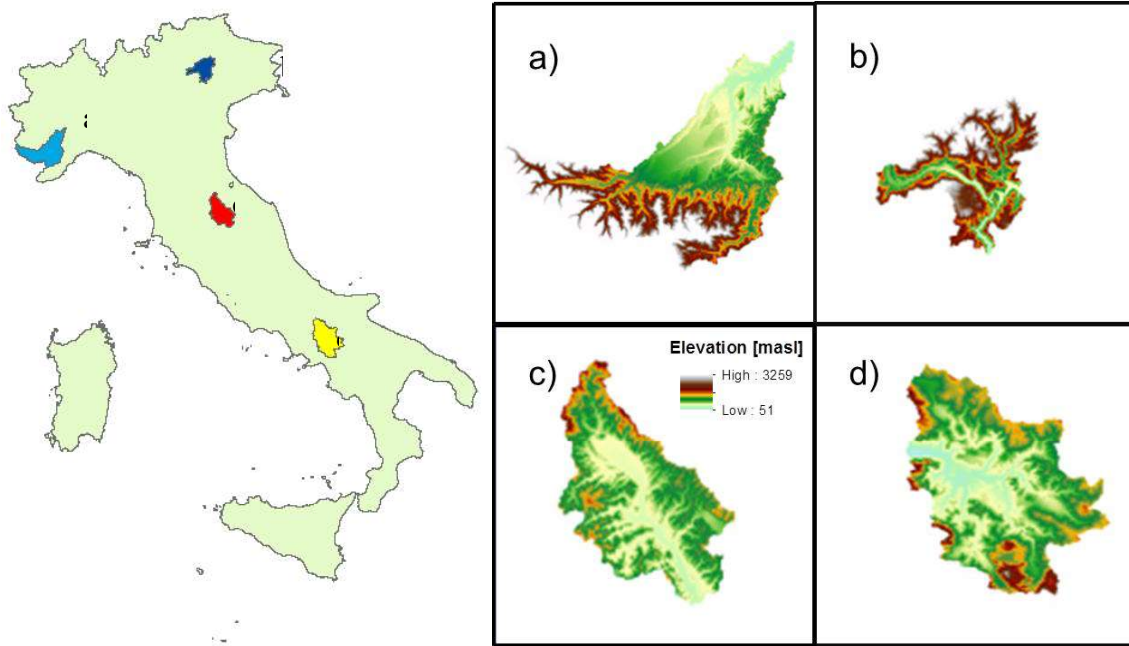
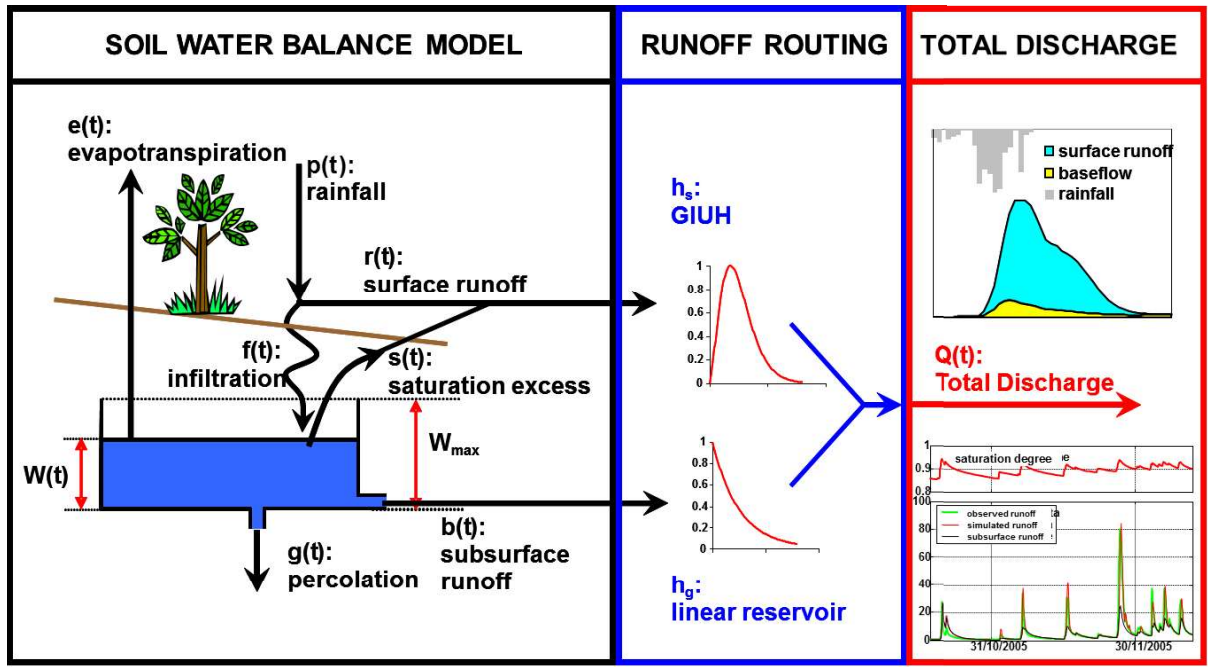


**Figure 1** – Geographical location and elevation of the a) Tanaro River basins, b) Brenta River basin, c) Tiber River basin and d) Volturno River basin (not in scale).

1  
2  
3  
4  
5  
6  
7  
8  
9  
10  
11  
12  
13  
14  
15  
16  
17  
18  
19  
20  
21  
22  
23  
24  
25  
26  
27  
28  
29  
30  
31  
32  
33  
34  
35  
36  
37  
38  
39  
40  
41  
42  
43  
44  
45  
46  
47  
48  
49  
50  
51  
52  
53  
54  
55  
56  
57  
58  
59  
60  
61  
62  
63  
64  
65



Figure

2 – Schematization of the MISDc rainfall-runoff model with the representation of the simulated hydrological processes.

1  
2  
3  
4  
5  
6  
7  
8  
9  
10  
11  
12  
13  
14  
15  
16  
17  
18  
19  
20  
21  
22  
23  
24  
25  
26  
27  
28  
29  
30  
31  
32  
33  
34  
35  
36  
37  
38  
39  
40  
41  
42  
43  
44  
45  
46  
47  
48  
49  
50  
51  
52  
53  
54  
55  
56  
57  
58  
59  
60  
61  
62  
63  
64  
65

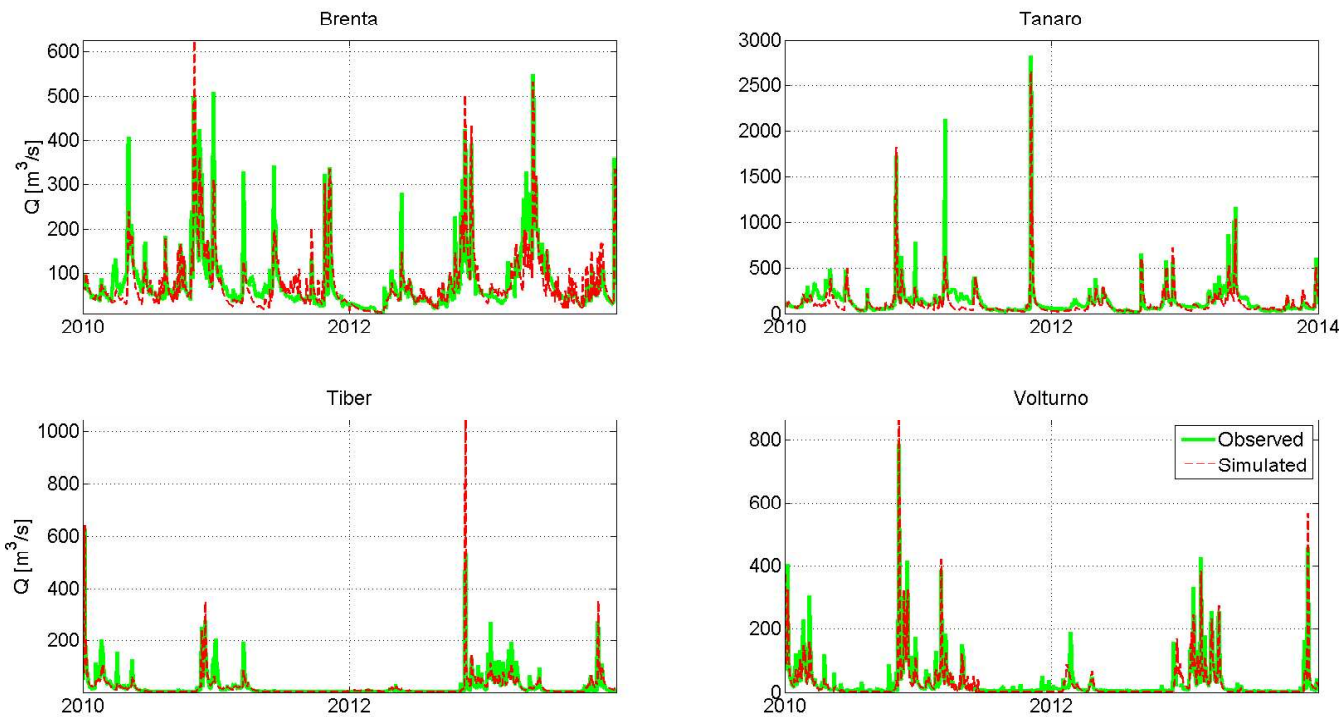


**Figure 3** – Comparison of observed and simulated discharge obtained by forcing MISDc model with ground observed rainfall for Brenta (up-left), Tanaro (up-right), Tiber (bottom-left) and Volturno (bottom-right) basins, during the entire analysis period (2010-2013).

1  
2  
3  
4  
5  
6  
7  
8  
9  
10  
11  
12  
13  
14  
15  
16  
17  
18  
19  
20  
21  
22  
23  
24  
25  
26  
27  
28  
29  
30  
31  
32  
33  
34  
35  
36  
37  
38  
39  
40  
41  
42  
43  
44  
45  
46  
47  
48  
49  
50  
51  
52  
53  
54  
55  
56  
57  
58  
59  
60  
61  
62  
63  
64  
65

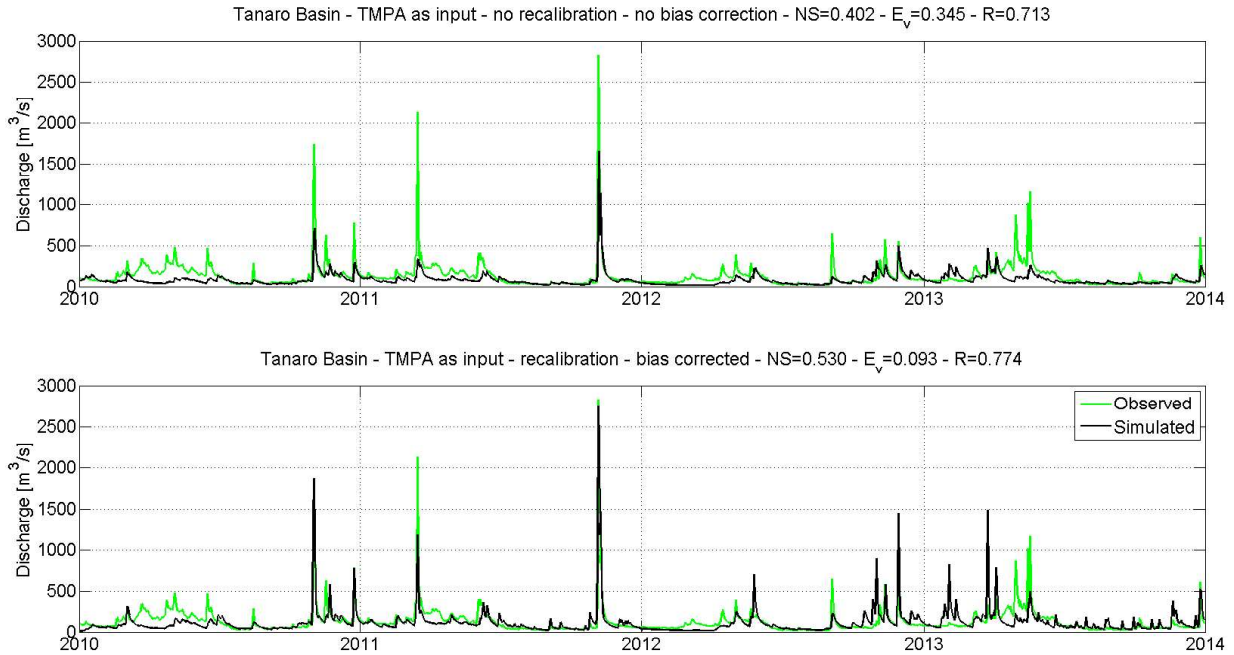


**Figure 4** – Observed and simulated hydrographs obtained by forcing MISDc model with TMPA data before (upper panel) and after (lower panel) bias correction and model recalibration.

1  
2  
3  
4  
5  
6  
7  
8  
9  
10  
11  
12  
13  
14  
15  
16  
17  
18  
19  
20  
21  
22  
23  
24  
25  
26  
27  
28  
29  
30  
31  
32  
33  
34  
35  
36  
37  
38  
39  
40  
41  
42  
43  
44  
45  
46  
47  
48  
49  
50  
51  
52  
53  
54  
55  
56  
57  
58  
59  
60  
61  
62  
63  
64  
65

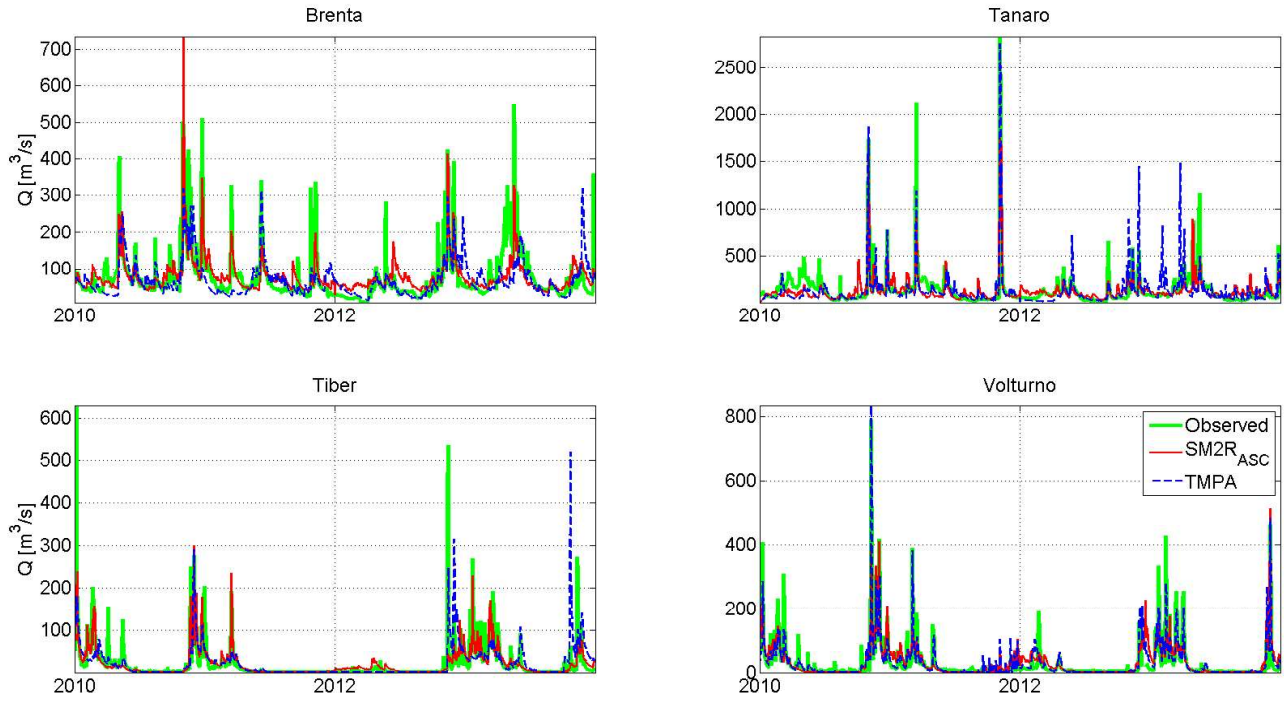


**Figure 5** – Comparison of observed and simulated daily discharge obtained by forcing MISDc model with the two satellite rainfall products SM2RASC and TMPA for Brenta (up-left), Tanaro (up-right), Tiber (bottom-left) and Volturno (bottom-right) basins, during the entire analysis period (2010-2013).

1  
2  
3  
4  
5  
6  
7  
8  
9  
10  
11  
12  
13  
14  
15  
16  
17  
18  
19  
20  
21  
22  
23  
24  
25  
26  
27  
28  
29  
30  
31  
32  
33  
34  
35  
36  
37  
38  
39  
40  
41  
42  
43  
44  
45  
46  
47  
48  
49  
50  
51  
52  
53  
54  
55  
56  
57  
58  
59  
60  
61  
62  
63  
64  
65

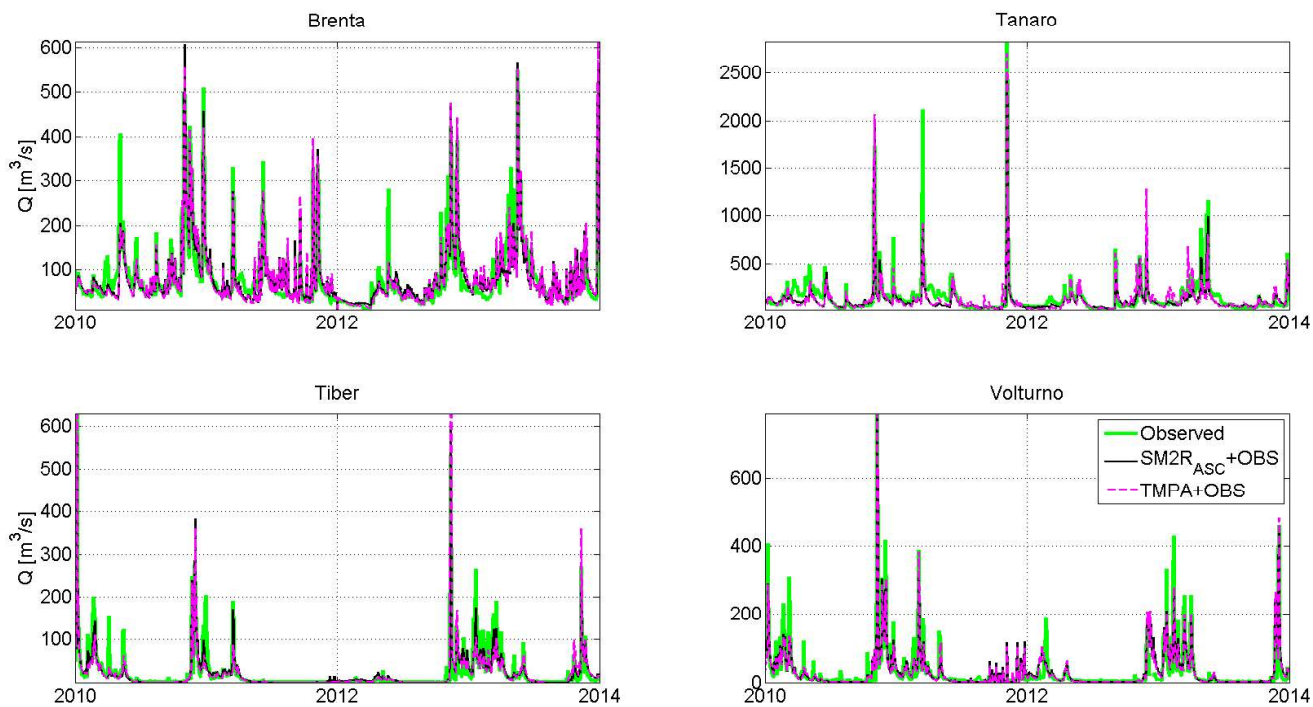


**Figure 6** – Comparison of observed and simulated daily discharge obtained by forcing MISDc model with the two integrated rainfall products SM2RASC+OBS and TMPA +OBS for Brenta (up-left), Tanaro (up-right), Tiber (bottom-left) and Voltorno (bottom-right) basins, during the entire analysis period (2010-2013).



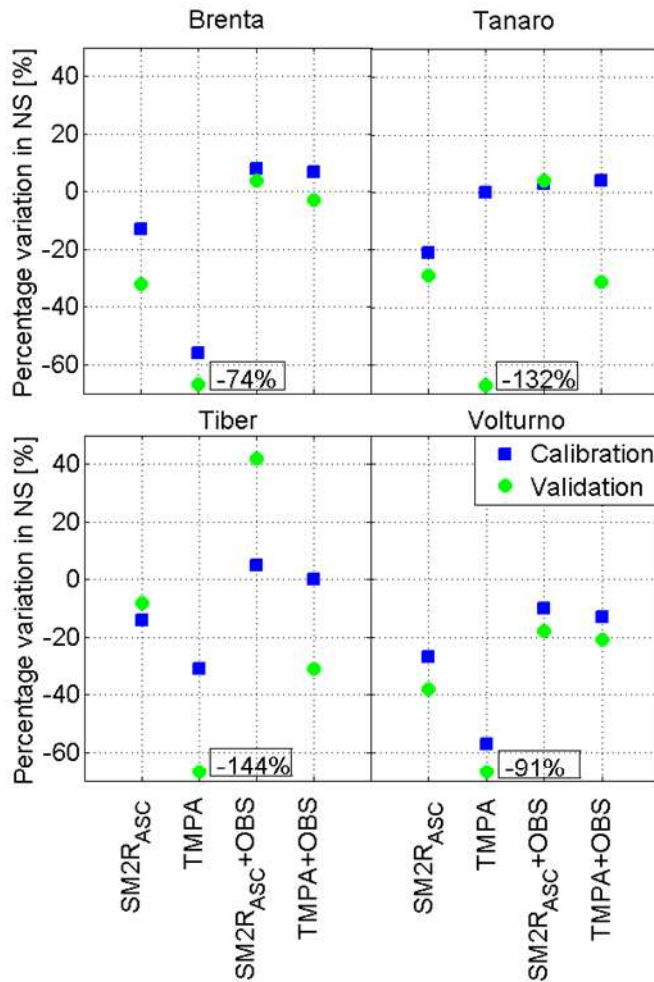


**Figure 7** – Nash-Sutcliffe efficiency index (*NS*) percentage variation obtained by forcing MISDc model with SM2RAIN derived rainfall (SM2RASC), TMPA 3B42-RT product (TMPA) and the integrated products between the observed and satellite rainfall data (SM2RASC+OBS and TMPA+OBS) during calibration (blue squares) and validation (green rumbles). The text boxes show the percentage variations in *NS* obtained for TMPA during the validation period that exceed the axis limit.



1  
2  
3  
4  
5  
6  
7  
8  
9  
10  
11  
12  
13  
14  
15  
16  
17  
18  
19  
20  
21  
22  
23  
24  
25  
26  
27  
28  
29  
30  
31  
32  
33  
34  
35  
36  
37  
38  
39  
40  
41  
42  
43  
44  
45  
46  
47  
48  
49  
50  
51  
52  
53  
54  
55  
56  
57  
58  
59  
60  
61  
62  
63  
64  
65

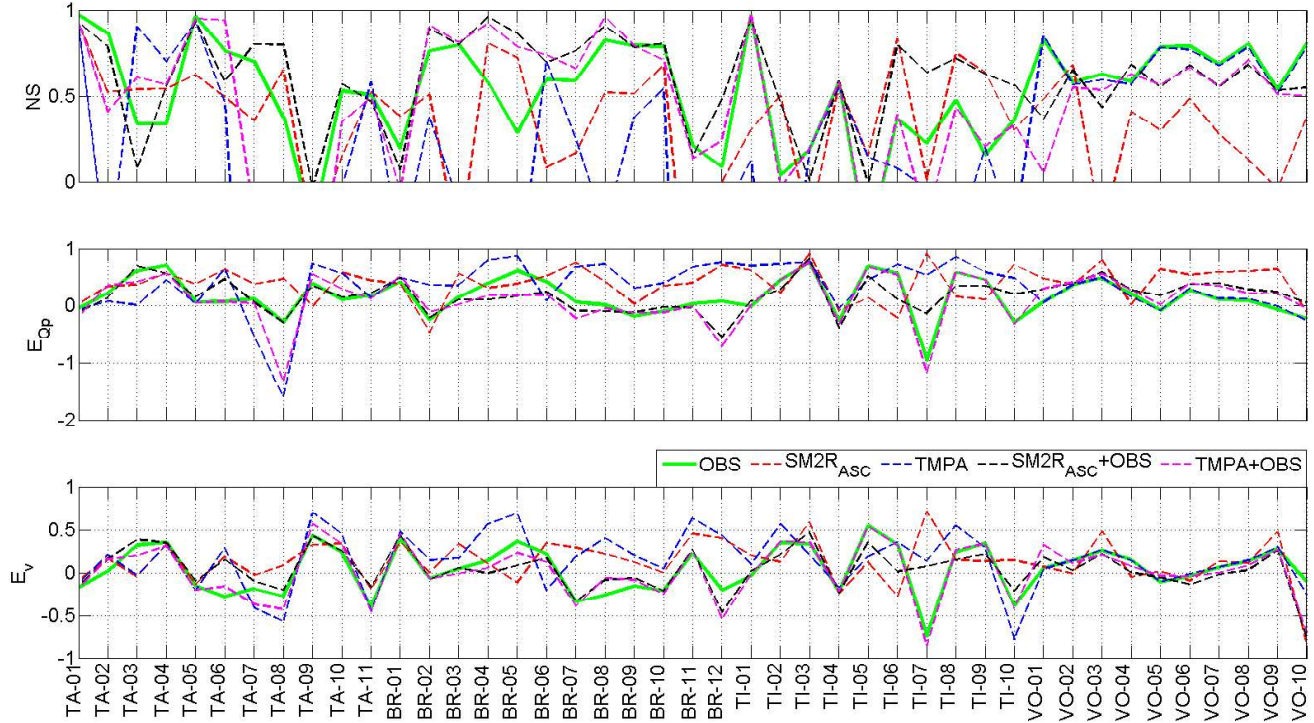


**Figure 8** – Performance scores obtained during the flood events simulations over the Tanaro (TA), Brenta (BR), Tiber (TI) and Volturno (VO) basins by forcing MISDc model with observed data (OBS, solid green line), SM2RAIN derived rainfall (SM2R<sub>ASC</sub>, dashed red line), TMPA data (TMPA, dashed blue line), integrated product between SM2R<sub>ASC</sub> and OBS data (SM2R<sub>ASC</sub>+OBS, dashed black line) and integrated product between TMPA and OBS data (TMPA+OBS, dashed magenta line). Nash-Sutcliffe efficiency index ( $NS$ , upper panel), percentage error in peak discharge ( $E_{Qp}$ , middle panel) and percentage error on direct runoff volume ( $E_v$ , bottom panel). In the upper panel graph, the y-axis is truncated to 0 for visualization purposes.

1  
2  
3  
4  
5  
6  
7  
8  
9  
10  
11  
12  
13  
14  
15  
16  
17  
18  
19  
20  
21  
22  
23  
24  
25  
26  
27  
28  
29  
30  
31  
32  
33  
34  
35  
36  
37  
38  
39  
40  
41  
42  
43  
44  
45  
46  
47  
48  
49  
50  
51  
52  
53  
54  
55  
56  
57  
58  
59  
60  
61  
62  
63  
64  
65

## TABLES

**Table 1** – Main characteristics of the investigated basins: gauging station, drainage area, Mean Annual Rainfall (MAR), Mean Annual Temperature (MAT), average elevation (in m a.s.l.) and average slope (in °).

<b>Basin</b>	<b>Gauging station</b>	<b>Area (km<sup>2</sup>)</b>	<b>MAR (mm)</b>	<b>MAT (°C)</b>	<b>Average altitude (m a.s.l.)</b>	<b>Average slope (°)</b>
Tanaro	Asti S. Martino	3229.7	1125	8.94	1025	15.59
Brenta	Berzizza	1506.3	2123.8	7.04	1239	22.53
Tiber	Ponte Felcino	1879	967.76	13.22	518	10.76
Volturno	Solopaca	2578.8	1208.1	13.33	543	8.80

1  
2  
3  
4  
5  
6  
7  
8  
9  
10  
11  
12  
13  
14  
15  
16  
17  
18  
19  
20  
21  
22  
23  
24  
25  
26  
27  
28  
29  
30  
31  
32  
33  
34  
35  
36  
37  
38  
39  
40  
41  
42  
43  
44  
45  
46  
47  
48  
49  
50  
51  
52  
53  
54  
55  
56  
57  
58  
59  
60  
61  
62  
63  
64  
65

**Table 2** – Correlation coefficients (*R*) and Root Mean Square Error (*RMSE*) for the analysed satellite products (SM2R<sub>ASC</sub> and TMPA) against observed rainfall during the calibration (CAL) and validation (VAL) periods.

Basin	SM2R <sub>ASC</sub>				TMPA			
	CAL		VAL		CAL		VAL	
	<i>R</i>	<i>RMSE</i>	<i>R</i>	<i>RMSE</i>	<i>R</i>	<i>RMSE</i>	<i>R</i>	<i>RMSE</i>
Brenta	0.56	14.97	0.49	14.91	0.70	12.78	0.66	13.55
Tanaro	0.60	7.56	0.48	6.96	0.79	5.94	0.69	6.52
Tiber	0.54	7.00	0.49	7.66	0.71	5.73	0.83	9.25
Volturno	0.63	6.10	0.60	5.80	0.64	6.07	0.63	5.78

1  
2  
3  
4  
5  
6  
7  
8  
9  
10  
11  
12  
13  
14  
15  
16  
17  
18  
19  
20  
21  
22  
23  
24  
25  
26  
27  
28  
29  
30  
31  
32  
33  
34  
35  
36  
37  
38  
39  
40  
41  
42  
43  
44  
45  
46  
47  
48  
49  
50  
51  
52  
53  
54  
55  
56  
57  
58  
59  
60  
61  
62  
63  
64  
65

**Table 3** – Nash-Sutcliffe efficiency (*NS*), correlation coefficient (*R*) and percentage volume error (*E<sub>v</sub>*) obtained by forcing MISDc hydrologic model with observed, satellite (SM2R<sub>ASC</sub> and TMPA) and integrated (SM2R<sub>ASC</sub>+OBS and TMPA+OBS) rainfall data, during the calibration (2010-2011) and validation (2012-2013) periods. In bold font the best performance scores of each basin are reported while the scores are in italic font if better than those obtained with ground observed rainfall (OBS). The highest performance of the integrated SM2R<sub>ASC</sub>+OBS product for Brenta, Tanaro and Tiber river basins is evident.

Basin	Calibration (2010-2011)			Validation (2012-2013)		
	<i>NS</i>	<i>R</i>	<i>E<sub>v</sub></i> (%)	<i>NS</i>	<i>R</i>	<i>E<sub>v</sub></i> (%)
<b>OBS</b>						
Brenta	0.72	0.86	6	0.76	0.88	4
Tanaro	0.76	0.89	23	0.68	0.83	11
Tiber	0.77	0.88	16	0.52	0.77	-15
Volturno	<b>0.86</b>	<b>0.93</b>	14	<b>0.77</b>	<b>0.88</b>	<b>5</b>
<b>SM2R<sub>ASC</sub></b>						
Brenta	0.63	0.73	-2	0.52	0.73	-4
Tanaro	0.60	0.78	<i>13</i>	0.48	0.70	<i>-10</i>
Tiber	0.66	0.81	<i>3</i>	0.48	0.70	<i>-1</i>
Volturno	0.63	0.79	-3	0.48	0.72	-32
<b>TMPA</b>						
Brenta	0.32	0.60	9	0.20	0.49	6
Tanaro	0.76	0.89	<i>19</i>	-0.22	0.49	-4
Tiber	0.53	0.73	16	-0.23	0.42	-27
Volturno	0.37	0.61	6	0.07	0.36	36
<b>SM2R<sub>ASC</sub>+OBS</b>						
Brenta	<b>0.78</b>	<b>0.89</b>	<i>1</i>	<b>0.79</b>	<b>0.88</b>	-5
Tanaro	<b>0.78</b>	0.89	<i>21</i>	<b>0.71</b>	<b>0.85</b>	9
Tiber	<b>0.81</b>	<b>0.90</b>	<i>10</i>	<b>0.74</b>	<b>0.86</b>	-6
Volturno	0.77	0.88	<i>1</i>	0.63	0.82	-34
<b>TMPA+OBS</b>						
Brenta	0.77	0.88	3	0.74	0.87	-4
Tanaro	0.79	<b>0.90</b>	20	0.47	0.73	<b>3</b>
Tiber	0.77	0.88	17	0.36	0.81	-14
Volturno	0.75	0.87	5	0.61	0.81	-26

1  
2  
3  
4  
5  
6  
7  
8  
9  
10  
11  
12  
13  
14  
15  
16  
17  
18  
19  
20  
21  
22  
23  
24  
25  
26  
27  
28  
29  
30  
31  
32  
33  
34  
35  
36  
37  
38  
39  
40  
41  
42  
43  
44  
45  
46  
47  
48  
49  
50  
51  
52  
53  
54  
55  
56  
57  
58  
59  
60  
61  
62  
63  
64  
65

**Table 4** – Integration coefficient (K) for the considered basins by using as model input the integrated products between the observed and satellite products (SM2RASC+OBS and TMPA+OBS).

<b>Basin</b>	<b>SM2R<sub>ASC</sub>+OBS</b>	<b>TMPA+OBS</b>
Brenta	0.8	0.9
Tanaro	0.8	0.5
Tiber	0.7	0.9
Volturno	0.8	0.9